Mechanism of ac conduction in nanostructured manganese zinc mixed ferrites

Mechanism of ac conduction in nanostructured manganese zinc mixed ferrites

E Veena Gopalan[1], **K A Malini**[2], **S Sagar**[1,3], **D Sakthi Kumar**[4],
Yasuhiko Yoshida[4], **I A Al-Omari**[5] **and M R Anantharaman**[1]

[1] Department of Physics, Cochin University of Science and Technology, Cochin 682 022, Kerala, India

[2] Department of Physics, Vimala College, Thrissur 680 009, Kerala, India

[3] Government Polytechnic College, Adoor, Manakkala, Pathanamthitta 691 551, Kerala, India

[4] Bio-Nano Electronics Research Centre, Department of Applied Chemistry, Toyo University, Kawagoe, Saitama 350-8585, Japan

[5] Department of Physics, College of Sciences, PO Box 36, Sultan Qaboos University, PC 123, Muscat, Sultanate of Oman

E-mail: mraiyer@gmail.com

Abstract

$Mn_{1-x}Zn_xFe_2O_4$ nanoparticles ($x = 0$ to 1) were synthesized by the wet chemical co-precipitation technique. X-ray diffraction and transmission electron microscopy and high resolution transmission electron microscopy were effectively utilized to investigate the different structural parameters. The ac conductivity of nanosized $Mn_{1-x}Zn_xFe_2O_4$ were investigated as a function of frequency, temperature and composition. The frequency dependence of ac conductivity is analysed by the power law $\sigma(\omega)_{ac} = B\omega^n$ which is typical for charge transport by hopping or tunnelling processes. The temperature dependence of frequency exponent n was investigated to understand the conduction mechanism in different compositions. The conduction mechanisms are mainly based on polaron hopping conduction.

(Some figures in this article are in colour only in the electronic version)

1. Introduction

The study of transition metal oxides, particularly spinel ferrites in the nanoregime, assumes significance from a fundamental point of view as well as an applied perspective. The high permeability and resistivity values of mixed ferrites, namely Ni–Zn ferrite and Mn–Zn ferrite are used in high quality filters, transformer cores, radio frequency circuits, rod antennas, read/write heads in high speed digital tapes and other devices [1–3]. The structural, magnetic and electrical properties of ferrites are found to be sensitive to their composition and microstructure, which in turn are dependent on the processing conditions [4]. Although the electrical and magnetic properties of ferrites in the micrometre regime have been well studied, leading to several applications, a thorough understanding of their electrical properties in the nanoregime is lacking. There are numerous reports with regard to the finite size effects on the structural and magnetic properties of ferrite nanoparticles

[5–8]. However, there exist only a few systematic studies on the electrical properties of ferrites in the nanoregime [9].

Measurements on frequency dependent ac conductivity are useful techniques to characterize the transport process in ferrites. It was thought that electrical conduction in ferrites results from the thermal activation of electrons or positive holes in the ionic lattice. The activation energy for electrical conduction is considerably reduced if the crystal lattice intrinsically contains cations of one element in more than one valence state. In mixed ferrites, the conductivity is found to be dependent on the availability of Fe^{2+}/Fe^{3+} ions and M^{2+}/M^{3+} pairs in octahedral sites. Thus, cation distribution along with their characteristic oxidation states play a dominant role in the conduction process. The cation distribution is distinctly different in ferrite nanoparticles compared with the bulk. The presence of Mn^{3+} ions along with Mn^{2+} ions will also affect the cation distribution in these ferrites. In zinc substituted $Mn_{1-x}Zn_xFe_2O_4$, the zinc ions are likely to occupy

J. Phys. D: Appl. Phys. **42** (2009) 165005

E Veena Gopalan *et al*

the tetrahedral sites. In the case of samples prepared using ceramic techniques, the zinc ions were found to exist only in the tetrahedral sites (A sites) [10]. The occupancy of zinc ions in octahedral sites in the nanoregime has a direct dependence on the cation distribution [11–13]. All these factors are bound to play a major role in deciding the overall electrical properties of the nanosized manganese zinc ferrite.

A detailed investigation on the transport properties of nanoparticles belonging to a series of the type $Mn_{1-x}Zn_xFe_2O_4$ mixed ferrite can throw light on the mechanism of electrical conduction in nanosized mixed ferrites. This is possible by subjecting these materials to conductivity studies in the ac regime over a wide range of frequencies. For this, nanosized $Mn_{1-x}Zn_xFe_2O_4$ were synthesized by the chemical co-precipitation method. The variation of ac conductivity with frequency and temperature is studied. The ac conduction mechanism is then analysed using existing models. The effect of zinc substitution on the ac electrical conductivity is also investigated in detail and reported here.

2. Experimental

Manganese zinc ferrites belonging to the series of $Mn_{1-x}Zn_xFe_2O_4$ ($x = 0$ to 1 in steps of 0.2) were synthesized by wet chemical co-precipitation under similar conditions. Aqueous solutions of $(1 - X)$ molar manganese chloride ($MnCl_2 \cdot 4H_2O$) and X molar zinc chloride ($ZnCl_2 \cdot$ anhydrous) and two molar ferric chloride ($FeCl_3 \cdot$ anhydrous) were mixed to form a solution. This mixture solution was poured quickly into boiling 10M NaOH solution diluted in 1800 ml of water under vigorous stirring. The formation of precipitate was found to be in the pH range 12.5–13. The solution was kept at 90 °C for 40 min under vigorous stirring. The precipitate was washed several times with distilled water, then filtered and dried in an oven. These powder samples were then pressed into pellets having a diameter of 12 mm and around a 2 mm thickness under an isostatic pressure of 5 ton. These pellets were then heat treated at 200 °C before being subjected to different studies. Uniformity in heat treatment, pressure applied was ensured for all the samples in the series.

These samples were characterized using x-ray powder diffractometer (Rigaku D max-C) using Cu Kα radiation ($\lambda = 1.5405$ Å). Lattice parameter of these samples of different compositions was calculated assuming cubic symmetry. The average crystallite size of each sample was estimated by employing the Debye–Scherrer formula. The particle size was estimated by subjecting the samples to transmission electron microscopy (TEM) studies (Joel JEM-2200 FS). Hysteresis loop parameters at room temperature were evaluated by using a vibrating sample magnetometer. (Model: EG&G PAR 4500). Scanning electron microscopy was employed to check the morphology of the pelletized samples (JSM-6335 FESEM).

Dielectric measurements were carried out on these samples using a home made dielectric cell and an HP 4285 LCR meter in the frequency range of 100 KHz–8 MHz over a temperature of 303–403 K. Copper discs of the same diameter were used as contact electrodes and the measurements were
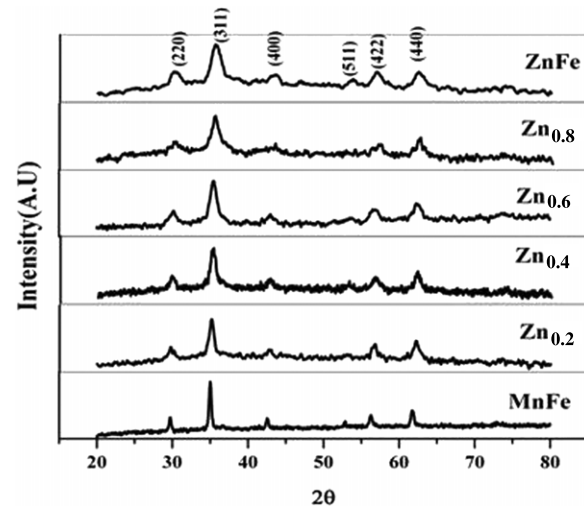

Figure 1. XRD Pattern of $Mn_{1-x}Zn_xFe_2O_4$.

Table 1. Structural and magnetic characteristics of $Mn_{1-x}Zn_xFe_2O_4$.

$Mn_{1-x}Zn_xFe_2O_4$ (X)	Particle size (nm)	Magnetization (M) at 300 K (at 13.5 kOe) (emu g^{-1})
0	29.1	57
0.2	14.7	56
0.4	12.9	53
0.6	10.3	31
0.8	8.2	7.5
1	7.2	5.2

carried out under rotary vacuum. Lead and fringe capacitance were eliminated before every run of the sample.

The ac conductivity of these samples were evaluated using the relation

$$\sigma_{ac} = 2\pi f \tan \delta \varepsilon_0 \varepsilon_r, \qquad (1)$$

where f is the frequency of the applied field, $\tan \delta$ is the loss factor and ε_r, the real part of the dielectric constant. The data acquisition was automated by interfacing the LCR meter with LabView. The details are cited elsewhere [14]. The details of the measurement and analysis of dielectric dispersion and absorption are described elsewhere [15].

3. Results and discussion

3.1. Structural and magnetic characterization

The x-ray diffraction patterns of mixed ferrites belonging to the series $Mn_{1-x}Zn_xFe_2O_4$ is depicted in figure 1. They are found to be characteristic of a spinel structure. The particle size of the different compositions is evaluated using the Debye–Scherer formula and shown in table 1. Further the particle size was estimated using TEM and was found to be in good agreement with those obtained from line broadening analysis of x-ray diffraction. The reduction in particle size with zinc concentration is clearly evident from TEM images. (figures 2 and 3).

Scanning electron micrographs of the samples are depicted in figures 4 and 5. It can be seen that the grains are uniformly sized and are in the nanoregime. The micrographs
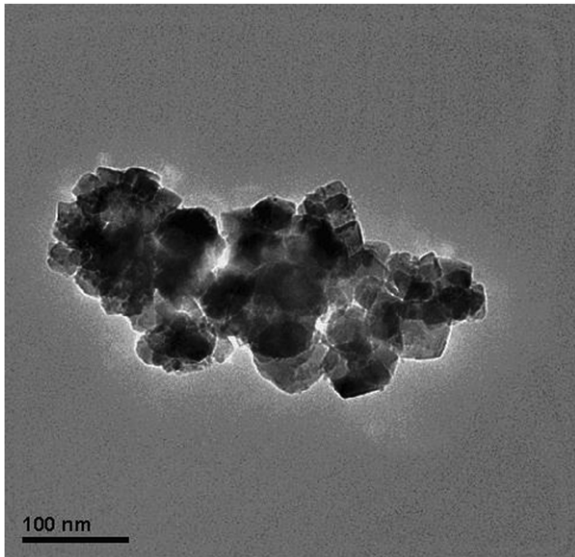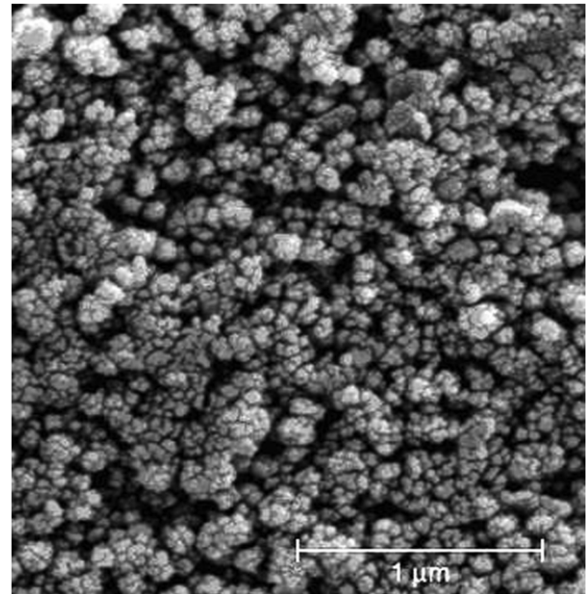
Figure 2. TEM image of $MnFe_2O_4$.

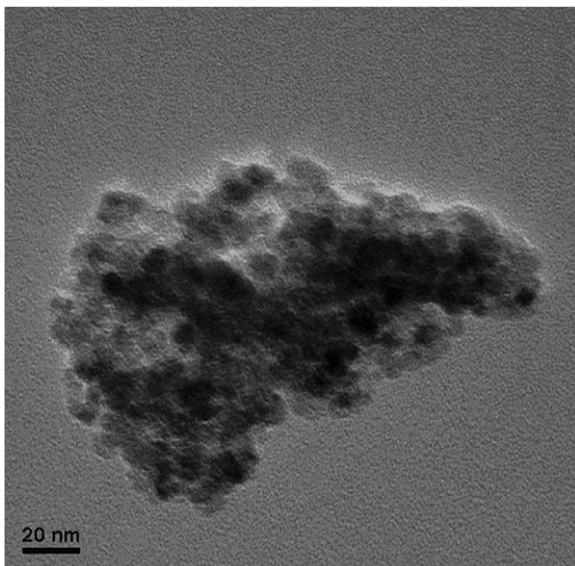

Figure 4. SEM image of $MnFe_2O_4$.
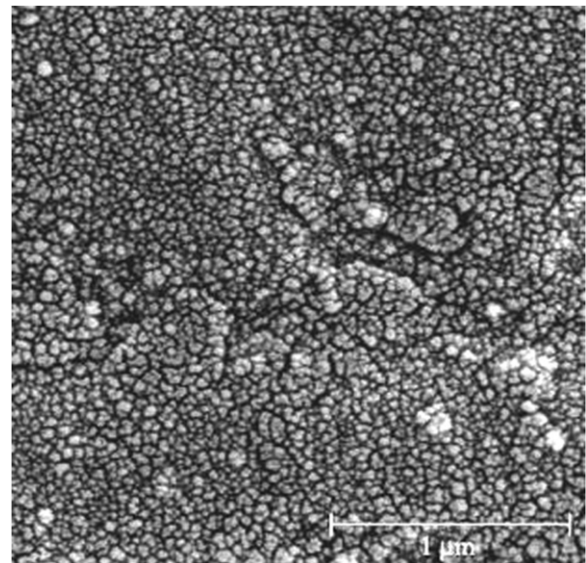

Figure 3. TEM image of $ZnFe_2O_4$.

Figure 5. SEM image of $ZnFe_2O_4$.

show the presence of a large number of interfaces which have a direct bearing on the dielectric properties of these ferrites. Representative hysteresis curves for $Mn_{1-x}Zn_xFe_2O_4$ at room temperature are portrayed in figure 6. The magnetization values are tabulated and are shown in table 1. The magnetic properties of nanosized $Mn_{1-x}Zn_xFe_2O_4$ do not comply with those of the same ferrite prepared in the micrometre regime. The magnetic properties were found to be different with respect to their bulk counterparts. The details are given elsewhere [16].

3.2. Ac conductivity studies in $Mn_{1-x}Zn_xFe_2O_4$

The variation of ac conductivity with frequency and temperature is given in figures 7(*a*)–(*f*). It is observed that initially the ac conductivity increases with frequency, reaches a maximum and then decreases. As the frequency of the applied field increases, hopping of charge carriers also increases,

thereby increasing the conductivity. But at higher frequencies, the hopping of charge carriers could not follow the applied field frequency and it lags behind the applied frequency resulting in a decrease in the ac conductivity values. The increase in ac conductivity with frequency and temperature could also be explained on the basis of the Koops model which assumes that ferrite samples act as a multilayer capacitor [17, 18]. According to this model, at low frequencies, the conductivity is due to the grain boundaries while the dispersion at higher frequencies is due to the conducting grains.

Ac conductivity decreases with zinc concentration, indicating a decrease in the availability of charge carriers with increasing zinc content (figure 8) With increasing zinc content there is a decrease in manganese ions (Mn^{3+}) and consequently the presence of Fe^{2+} ions in the octahedral sites is also reduced. Hence the number of Mn^{3+}–Mn^{2+} and Fe^{2+}–Fe^{3+}
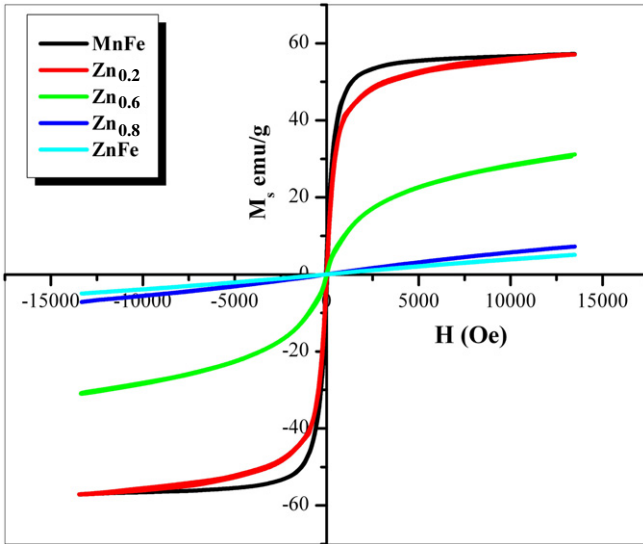
Figure 6. Room temperature hysteresis curves of $Mn_{1-x}Zn_xFe_2O_4$.

pairs available for hole and electron hopping will be less in number as the zinc content is increased. As a result, hopping decreases and charged species accumulate on the grain boundaries. Therefore, the resistance of the grain boundary increases and hence the probability of charged species crossing over the grain boundaries decreases. This eventually reduces conductivity with increasing zinc substitution. So there is a relatively large number of hopping pairs in manganese ferrite compared with the other compositions. In the case of zinc ferrite the presence of hopping pairs may be entirely due to the presence of zinc ions in the octahedral sites which give rise to electron hopping Fe^{2+}–Fe^{3+} pairs. It is interesting to see that (figures 7(a)–(f)) in manganese rich compositions, the increase in ac conductivity with temperature in the kilohertz region is diminutive while in the case of zinc rich samples there is a marked increase in conductivity with temperature in this regime. Hence different conduction mechanisms can be expected in these compositions.

The real part of ac electrical conductivity consists of two terms [19]:

$$\sigma = \sigma_1(T) + \sigma_2(\omega, T) \qquad (2)$$

The first term is the temperature dependent dc conductivity which is related to the drift of electric charge carriers and follows the Arrhenius relation. The second term is the frequency and temperature dependent part of the ac conductivity. From the Arrhenius relation, the activation energy at different frequencies can be found by plotting $\ln \sigma_{ac}$ versus temperature (figure 9). From the slope of the linear region of the graph, the activation energy (E_a) for electrical conduction at 4 MHz is determined. The variation of activation energy with zinc content indicates an increasing trend with increasing zinc content (figure 10). Since both hole hopping between Mn^{3+}–Mn^{2+} and Fe^{2+}–Fe^{3+} electron hopping can happen in these ferrites, the activation energy calculated can be taken as an average of the activation energies for the two hopping processes and should be less than 0.21 eV. Higher values of activation energy points towards polaron conduction

in these materials [20]. In ferrites, the cations are surrounded by close packed oxygen anions and hence can be treated as isolated from each other. There will be little direct overlap of the charge clouds or orbitals. Hence a localized electron model is appropriate in the case of electrons. When the charge carriers are localized, charge transport takes place via phonon assisted hopping between localized sites. Localization of the charge carriers may give rise to the formation of polarons and the charge transport may be considered between the nearest neighbour sites [21].

The temperature and frequency dependent ac conductivity in equation (2) which is related to the dielectric relaxation caused by the localized charge carriers is given by the power law [22]

$$\sigma_2(\omega, T) = B(T)\omega^n(T), \qquad (3)$$

where B is the parameter having the unit of conductivity and n is a dimensionless parameter.

Since ac conductivity is frequency dependent in the lower temperature region the power law (equation (3)) can be applied to the experimental data by plotting $\log \sigma_{ac}$ with $\log \omega$ for different compositions. This is done for the frequency region where σ_{ac} is exhibiting an increase with frequency. The value of n is estimated from the slope of the $\log \sigma_{ac}$ versus $\log \omega$ graphs. The conduction mechanism can be analysed on the basis of variation of the frequency component n with temperature [23, 24]. The dependence of n with temperature is plotted and is shown in figures 11(a)–(f). It can be seen that the behaviour of n is different in the manganese rich and zinc rich compositions. This observation indicated a different conduction mechanism in these compositions.

In manganese rich compositions of the series $Mn_{1-x}Zn_xFe_2O_4$ for $x \leqslant 0.5$ the value of n is found to be increasing with temperature (figures 11(a)–(c)).This is characteristic of small polaron tunnelling and can be explained based on the small polaron tunnelling model for ac conduction [25].

The frequency exponent n based on this model is evaluated as

$$n = 1 - \frac{4}{\ln (1/\omega\tau_0) - (W_H/k_B T)}, \qquad (4)$$

where k_B is Boltzmann's constant, T the temperature, W_H is the barrier height for infinite site separation, τ_0 the relaxation time and ω the angular frequency.

According to this model, the ac conductivity is given by

$$\sigma(\omega) = \frac{\pi^4}{24} \frac{e^2 k_B T [N(E_F)]^2 \omega R_\omega^4}{\alpha}, \qquad (5)$$

where e is the electronic charge, k_B is Boltzmann's constant, T is the temperature and α the spatial extent of polaron, $N(E_F)$ the density of states at the Fermi level and R_ω is the tunnelling distance.

However in the case of zinc rich compositions of $Mn_{1-x}Zn_xFe_2O_4$ up to Zn = 0.8 the variation of n is found to be different (figures 11(d)–(e)). The value of n decreases with temperature, reaches a minimum and then increases. This behaviour is in accordance with the variation of n in
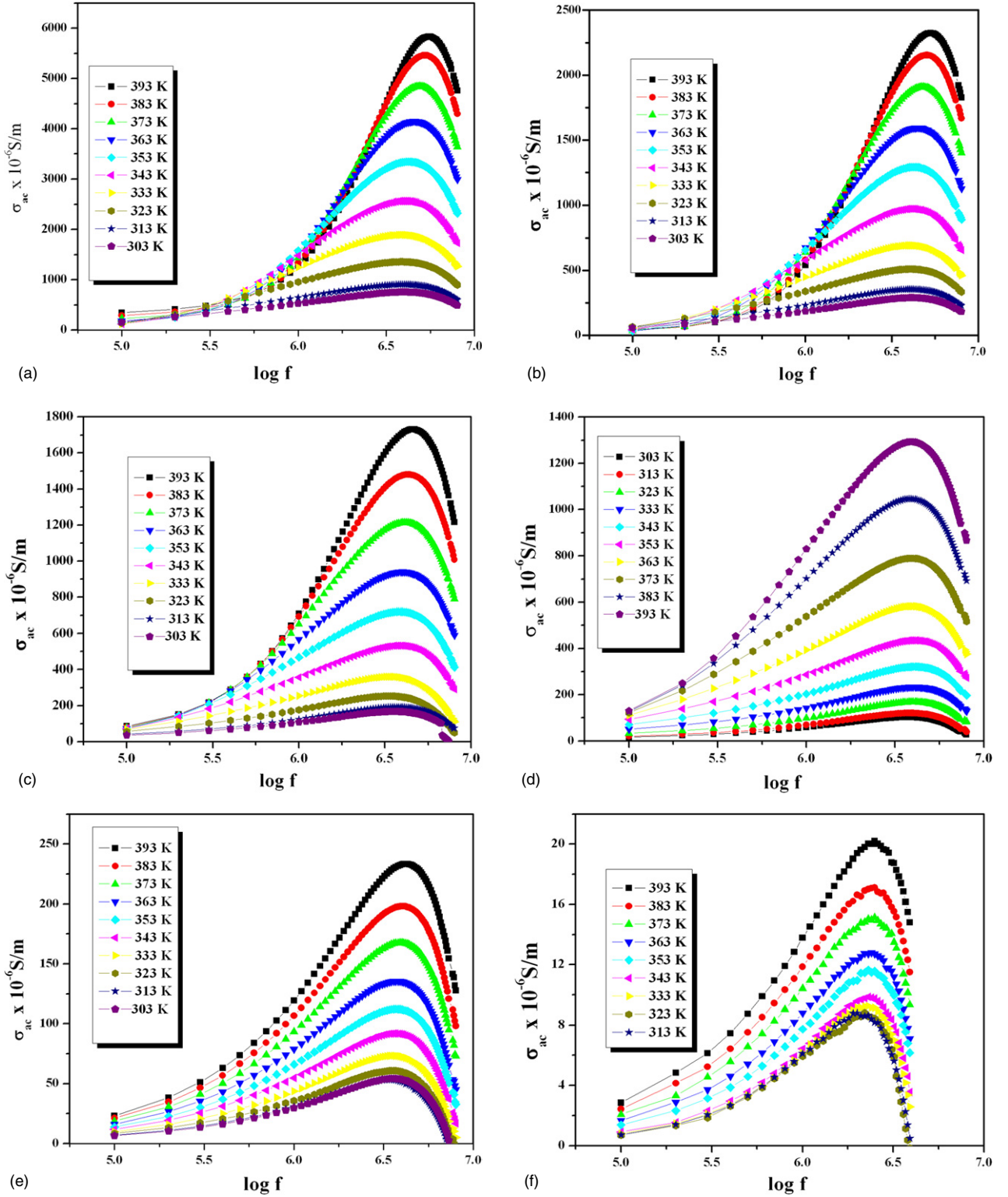
J. Phys. D: Appl. Phys. **42** (2009) 165005

E Veena Gopalan *et al*

Figure 7. Variation of ac conductivity with frequency and temperature of $Mn_{1-x}Zn_xFe_2O_4$: (*a*) MnFe, (*b*) $Zn_{0.2}$, (*c*) $Zn_{0.4}$, (*d*) $Zn_{0.6}$, (*e*) $Zn_{0.8}$ and (*f*) ZnFe.

the overlapping large polaron tunnelling model (OLPT) of ac conduction [26].

The frequency exponent n is given by the equation

$$n = 1 - \frac{8\alpha R_\omega + 6\beta W_{HO}r_p/R_\omega}{(2\alpha R_\omega + \beta W_{HO}r_p/R_\omega)^2}, \qquad (6)$$

where β is $1/k_BT$, k_B is Boltzmann's constant, T is the temperature in degree absolute, r_p is the polaron radius, separation and W_{HO} is the barrier height for infinite site separation, α is the spatial extent of the polaron, $N(E_F)$ is the density of states at the Fermi level and R_ω is the tunnelling distance.
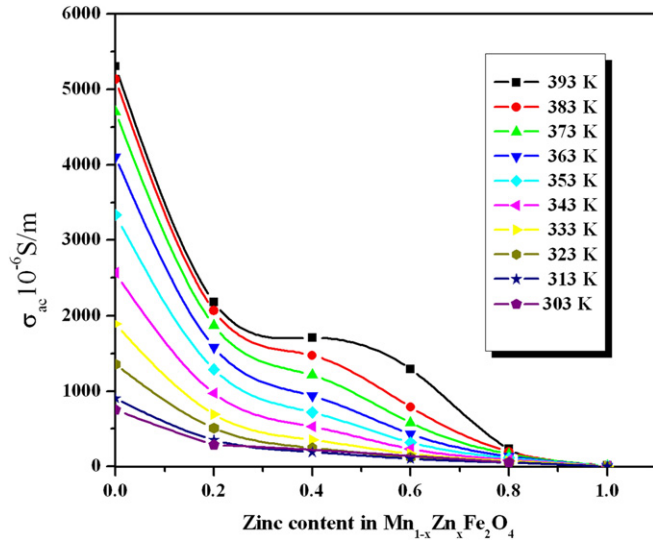
Figure 8. Variation of σ_{ac} with zinc content in $Mn_{1-x}Zn_xFe_2O_4$ at 4 MHz.
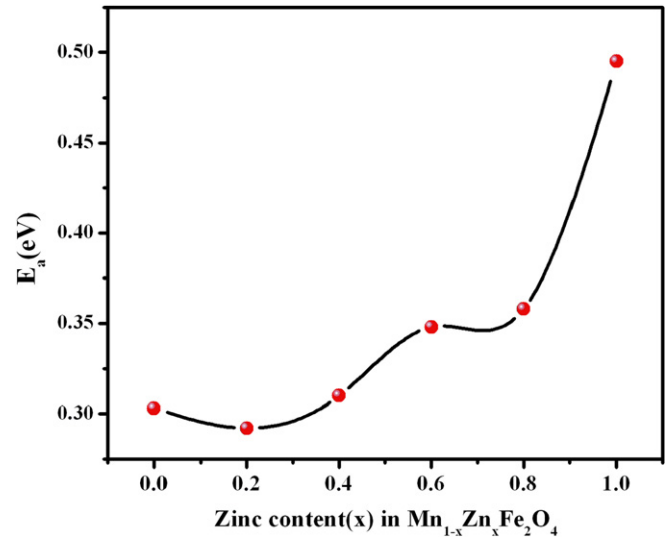
Figure 10. Variation of activation energy with zinc content.

where $N(E_F)$ is the density of states at the Fermi level, ε is the dielectric permittivity of the medium, ε_0 is the free space permittivity and R_ω is the hopping distance.

It has been found that apparently the mechanism of ac conduction in nanostructured manganese zinc ferrites is found to be different for different compositions. The formation of small non-overlapping polarons in the manganese rich compositions may be directly related to the availability of more hopping charge pairs in these ferrites. When there is a reduced number of hopping charges, the spatial extent of the polaron may extend to several interatomic distances resulting in the formation of overlapping large polarons. Hence OLPT conduction is observed in the zinc rich compositions. Since pristine zinc ferrite is free of Mn^{2+}–Mn^{3+} pairs, it is to be expected that in $ZnFe_2O_4$, the conductivity is predominating because of Fe^{3+}–Fe^{2+} electron hopping in the lattice. But the formation of these hopping ion pairs depends on the occupancy of Zn^{2+} ions in the octahedral sites preferentially. So the observed conduction mechanism in zinc ferrite is correlated barrier hopping conduction based on hopping of charge carriers between two sites over a barrier separating them. A clear understanding of the conduction mechanism in nanostructured ferrites remains elusive unless and until the conductivity measurements are carried out for a wide range of frequencies and over a wide temperature range.
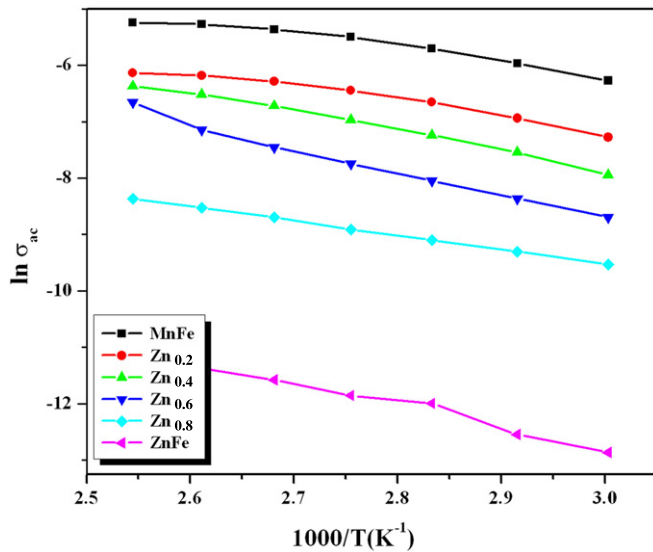

Figure 9. $\ln \sigma_{\mathrm{ac}}$ versus 1000/T $Mn_{1-x}Zn_xFe_2O_4$ at 4 MHz.

The ac conductivity for the OLPT model is given by [27]

$$\sigma(\omega) = \frac{\pi^4 e^2 (k_B T)^2 [N(E_F)]^2 \omega R_\omega^4}{12 \left(2\alpha k_B T + \left(W_{\mathrm{HO}} r_p / R_\omega^2\right)\right)}. \quad (7)$$

The maximum resistivity is observed in the case of zinc ferrite where a decrease in n with temperature is found (figure 11(f)). This variation of n with temperature is similar to that predicted by the correlated barrier hopping conduction model using the equation [28]

$$n = 1 - \frac{6k_B T}{W_M + k_B T \ln(\omega \tau_0)}. \quad (8)$$

The correlated barrier hopping model predicts ac conductivity as

$$\sigma(\omega) = \frac{\pi^3}{24} [N(E_F)]^2 \varepsilon \varepsilon_0 \omega R^6 \omega, \quad (9)$$

4. Conclusions

The ac conductivity of mixed ferrites belonging to the series $Mn_{1-x}Zn_xFe_2O_4$ were measured and it was found that ac conductivity decreased with increasing zinc content. This was confirmed by an increase in activation energy with zinc substitution. The higher values of activation energy indicated a conduction mechanism involving hopping of polarons. The frequency dependent term of ac conductivity was analysed and the frequency parameter n for different compositions were evaluated. Based on the variation of n with temperature, different mechanisms of conduction are found to exist in
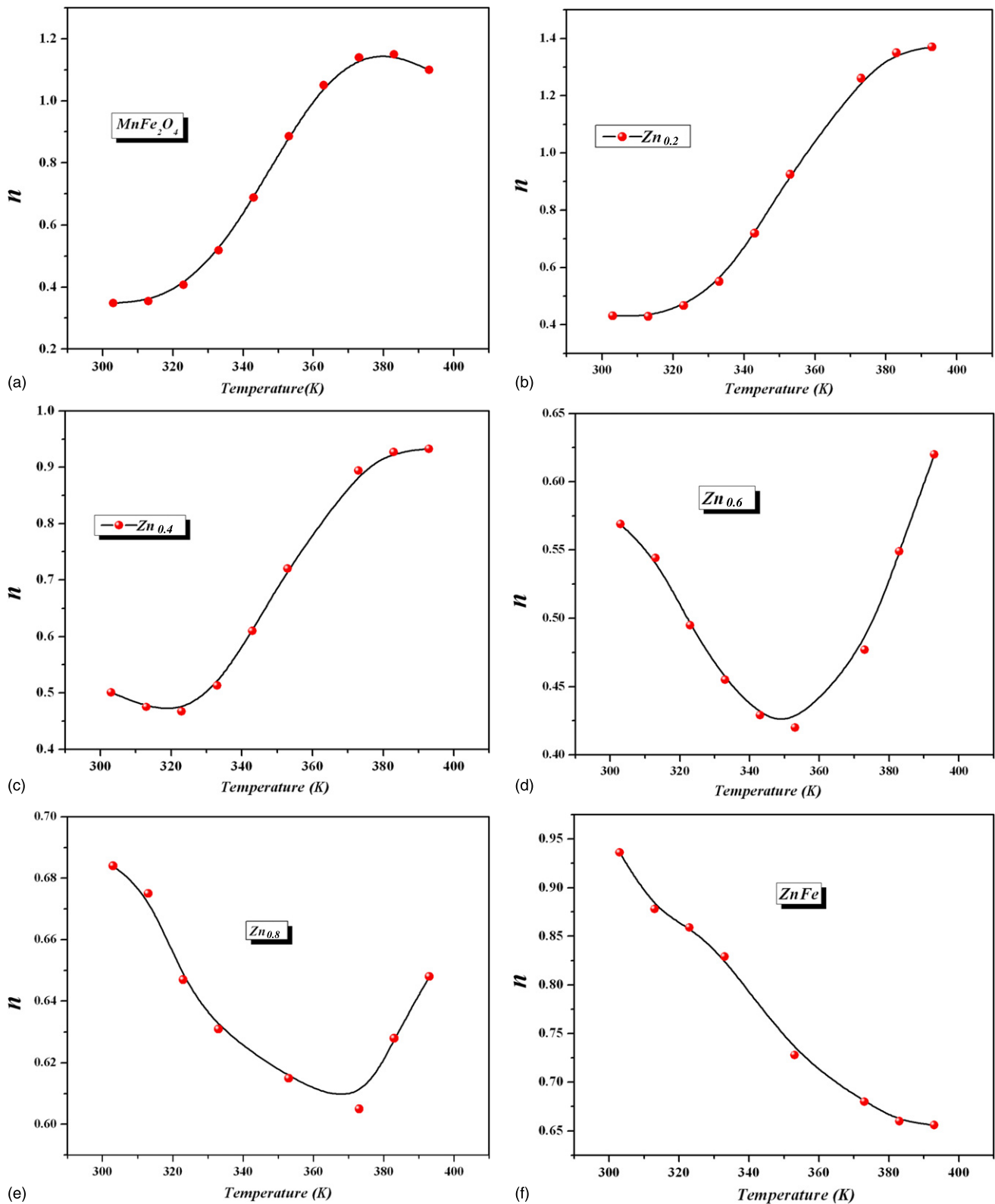
J. Phys. D: Appl. Phys. **42** (2009) 165005

E Veena Gopalan *et al*

Figure 11. Variation of *n* with temperature of $Mn_{1-x}Zn_xFe_2O_4$: (*a*) MnFe, (*b*) $Zn_{0.2}$, (*c*) $Zn_{0.4}$, (*d*) $Zn_{0.6}$, (*e*) $Zn_{0.8}$ and (*f*) ZnFe.

these compositions. Hence the conductivity behaviour of nanostructured $Mn_{1-x}Zn_xFe_2O_4$ can be suitably tuned by varying the concentration of zinc substitution. Subsequently, these mixed ferrites can be properly exploited for possible technological applications.

Acknowledgments

References

[1] Ott G, Wrba J and Lucke R 2003 *J. Magn. Magn.Mater.* **254** 535–7

[2] Ni S M and Lwin K T 2008 *Proc. World Academy of Science, Engineering and Technology (Bangkok, Thailand, 17–19 December 2008)* vol 36, ISSN 2070-3740

[3] Stanciulea L, Neamtu J, Feder M, Segal E, Cristea P and Gal L 1992 *J. Mater. Sci. Lett.* **11** 961

[4] Guyot M 1980 *J. Magn. Magn. Mater.* **18** 925–6

[5] Tang Z X, Chen J P, Sorenson C M, Klabunde K J and Hadjipanayis G C 1991 *Phys. Rev. Lett.* **67** 3602–5

[6] Hendriksen P V, Linderoth S and Lindgard P A 1993 *Phys. Rev. B* **48** 7259–73

[7] Rath C, Mishra N C, Anand S, Date S K, Das R P, Kulkarni S D and Sahu K K 2002 *J. Appl. Phys.* **91** 2211–5

[8] Rath C, Mishra N C, Anand S, Das R P, Sahu K K, Upadhyay C and Verma H C 2000 *Appl. Phys. Lett.* **76** 475–7

[9] Baruwati B, Madhusudan Reddy K, Manorama S V, Singh R K and Prakash O 2004 *Appl. Phys. Lett.* **85** 2833–5

[10] Craik D J 1975 *Magnetic Oxides—Part 1* (New York: Wiley)

[11] Shenoy S D, Joy P A and Anantharaman M R 2004 *J. Magn. Magn. Mater.* **269** 217–26

[12] Anantharaman M R *et al* 1998 *J .Magn. Magn. Mater.* **189** 83–8

[13] Lotgering F K 1966 *J. Phys. Chem. Solids* **27** 139–45

[14] Sindhu S, Anantharaman M R, Thampi B P, Malini K A and Kurian P 2002 *Bull. Mater. Sci.* **25** 599–607

[15] Veena Gopalan E, Malini K A, Sakthi Kumar D, Yoshida Y, Al-Omari I A, Saravanan S and Anantharaman M R 2009 *J. Phys.: Condens. Matter* **21** 146006

[16] Veena Gopalan E, Al-Omari I A, Malini K A, Joy P A, Sakthi Kumar D, Yoshida Y and Anantharaman M R 2009 *J. Magn. Magn. Mater.* **321** 1092–9

[17] Wagner K W 1913 *Ann. Phys. Lpz.* **40** 817–9

[18] Koops C G 1951 *Phys. Rev.* **83** 121–4

[19] Ahmed M A, El Hiti M A, El Nimr M K and Amer M A 1996 *J. Magn. Magn. Mater.* **152** 391–5

[20] Veena Gopalan E, Malini K A, Saravanan S, Sakthi Kumar D, Yoshida Y and Anantharaman M R 2008 *J. Phys. D: Appl. Phys.* **41** 185005

[21] Vishwanathan B and Moorthy V R K 1990 *Ferrite Materials: Science and Technology* (Berlin: Springer) p 10

[22] El Hiti M A 1996 *J. Phys. D: Appl. Phys.* **29** 501–5

[23] Elliot S R 1987 *Adv. Phys.* **36** 135–217

[24] Fayek M K, Mostafa M F, Sayedahmed F, Ata Allah S S and Kaiser M 2000 *J. Magn. Magn. Mater.* **210** 189–95

[25] Meaz T M, Attia S M and Abo El Ata A M 2003 *J. Magn. Magn. Mater.* **257** 296–305

[26] Ghosh A 1990 *Phys. Rev. B* **42** 1388–93

[27] Long A R 1982 *Adv. Phys.* **31** 553

[28] Elliot S R 1977 *Phil. Mag.* **36** 1291–304